International Journal of Scientific Research & Engineering Technology (IJSET)
Vol.23pp. 1-14

Assessment of Exposure to Airborne and Noise Pollution from Road Trafficin a High Mobility Urban Site Within the Sousse City Center

Ahmed Komti [#1], Abdessalem Jbara [#*2], Najah Kechiche [*3], Khalifa Slimi [#4]

[#] LESTE Laboratory, National Engineering School of Monastir, University of Monastir, Monastir, Tunisia
[*] Higher Institute of Transportation and Logistics of Sousse, University of Sousse, Sousse, Tunisia

Email 1 - ahmedkomti568@gmail.com
Email 2 - j.abdesslem@yahoo.fr
Email 3 - kechiche2000@gmail.com
Email 4 - khalifa_slimi@yahoo.fr

Abstract— **Road traffic contributes to the generation of air and noise pollution in urban areas, leading to adverse effects on human health. Therefore, accurately assessing exposure to air and noise pollution from road traffic is crucial for enhancing our comprehension of human health outcomes in epidemiological research. This paper aims to evaluate the simulation of road traffic pollutant dispersion and predict noise levels in a high-traffic area located within the city of Sousse. COPEERT software was used to estimate road emissions (based on vehicle numbers)., the nested mesoscale meteorology and micro-scale dispersion model system, GRAMM–GRAL V22.03, and The French NMPB-Roads-2008 model was chosen for predicting road noise levels. A Geographical Information System (GIS) was used to graphically represent the spatial distribution of noise emissions in the study area. During rush hour, exposure to traffic-related PM2.5 and PM10 pollutants is significantly higher for buildings located along the three busiest streets, with levels peaking at 30 and 20 µg.m^{-3}. PM2.5 and PM10 concentration levels fall, but they stay below 17 and 10 µg.m^{-3}, respectively, when there are no peak traffic times. The mean PM2.5/PM10 ratio is higher than 0.5 (0.58), which suggests that exhaust emissions, tire, and brake wear are the main causes of PM emissions. According to a road traffic noise analysis, the average noise level decreased by 3.69 dB(A) when the total traffic volume decreased by around 45%.**

Keywords— **Simulation, GRAMM–GRAL, Noise Level, QGIS, outdoor air pollution.**

I. INTRODUCTION

Driven by demographic expansion and economic prosperity, the demand for transportation has surged, leading to a notable increase in the number of motor vehicles utilizing road networks. As per the Tunisian Automotive Market Journal, the car fleet in Tunisia witnessed a substantial growth trajectory, rising from nearly 304,653 vehicles in the 1985 census to reach 2,331,972 vehicles by 2020 (Figure 1).

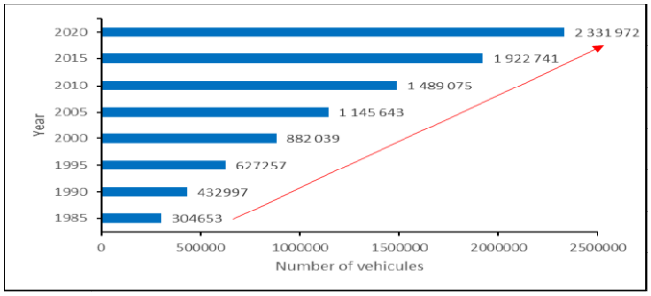

Figure 1 Evolution of the Tunisian car fleet from 1985 to 2020 [1].

They also provided data on the distribution of the Tunisian car fleet by category and age at the end of 2020. It was found that the category of vans represented almost a quarter of the total car fleet, while cars over 15 years old dominated, representing 52% from the total Tunisian car fleet (Figure 2) [1].

ISSN: 2356-5608

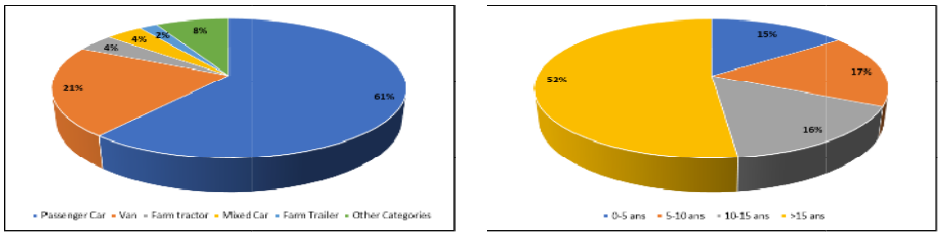

(a) (b)

Figure 2 Tunisian car fleet repartition by (a) category and (b) age at the end of year 2020 [1].

Despite its importance, noise pollution continues to be underestimated in many modern cities worldwide [2]. However, recent studies by Fallah-Shorshani et al [3] highlight a growing concern about traffic-related noise pollution. Effectively addressing this issue requires a comprehensive and coordinated effort by all stakeholders to achieve acceptable noise levels in different urban areas [4]. In addition, it's worth noting that ambient noise and air pollution often coincide and originate from similar sources, particularly traffic [5], raising further concerns as previous research has identified a spatial correlation between traffic-related noise and air pollution [6].

The livability of urban environments is influenced by various health and well-being effects associated with environmental exposures [7-9]. The main environmental health threat is air pollution, which is caused by human activities and causes approximately 400,000 premature deaths annually in Europe [10]. Exposures to factors like noise [11], heat [12], toxic chemicals [13], and heavy metals [14] have a significant impact on health negatively within urban areas, as 91% of the global population lacks access to clean air [15]. Everyday travel is a major source of daily exposure, as it exposes individuals to various and dynamic environmental variables [16]. Air pollution consists of a wide range of substances from different sources which may cause oxidative stress, local and systemic inflammation, respiratory system dysfunction, enhanced platelet activity and accelerated plaque formation [17]. There is increasing evidence linking noise to cardiometabolic disease, including MI (myocardial infarction). [18] Based on experimental and epidemiological evidence, proposed pathways from noise to cardiovascular disease include stress-induced activation of the hypothalamic-pituitary-adrenal axis and sleep disturbance. The noise generated by a vehicle can come from a variety of sources, the importance of which depends on the characteristics of the vehicle and the traffic conditions. Broadly, vehicle noise primarily stems from four main sources: mechanical noise associated with the powertrain (including intake, exhaust, and engine), rolling noise generated by tire-road contact, aerodynamic noise resulting from the interaction between the vehicle surface and airflow, and auxiliary sources such as brakes and horns [19]. An alternative to direct measurement of air pollutants is the use of modelling tools. These tools facilitate the understanding of phenomena, the extrapolation of existing measurements to areas lacking instrumentation and, importantly, the evaluation of operational solutions to control emissions and their impacts. These solutions may include changes in urban design, fuel composition, land use parameters and the implementation of alternative, intermodal or cleaner transport systems. Commonly used models for this purpose include the Operational Street Pollution Model (OSPM) [20], AERMOD [21], CALINE4 [22], ADMS-Urban [23] and SIRANE [24], and GRAMM/GRAL V22.03. [25], [26]. In this study, we have developed the initial inventory of pollutants released by traffic within the urban community of Sousse. Subsequently, we utilized the GRAMM/GRAL model to analyse the distribution of particulate matter (PM) across the region. The GRAMM/GRAL model is uniquely designed to facilitate long-term, city-wide simulations with detailed building resolution while maintaining computationally feasible costs. It operates by utilizing a discrete set of potential weather conditions along with corresponding steady-state flow and dispersion patterns, which are pre-computed and then synchronized hourly with real-time meteorological observations [27]. In recent years, there has been a marked increase in the development of more advanced and comprehensive models for calculating noise levels. Many of these models are tailored to specific regions or countries, such as ASJ in Japan [28], GIS in China [29], CORTN in the UK [30], CNR in Italy [31], RLS-90 in Germany [32], FHWA in the USA [33], Nord 2000 in the Nordic countries [34], StL-86 and SonRoad in Switzerland [35], ERTC in Thailand [36] and NMPB-roads in France [37]. In addition, models such as Harmonoise [38] and the latest addition, CNOSSOS-EU [39], have been developed specifically for the European Union.

It's important to note that CNOSSOS-EU has similarities with the NMBP-roads method in terms of sound propagation aspects. For a more comprehensive understanding and detailed comparison of these models, the reader is referred to an extended review in [40]- [45]. The Geographic Information System (GIS) has become increasingly

ISSN: 2356-5608

popular and serves as a crucial assessment tool in ecological environment evaluation [46]. Therefore, QGIS was employed in this research to produce noise maps [47] and visually interpret the areas most affected by pollution. This was accomplished by analysing measured noise levels (Leq) both during rush and non-rush hour, and by creating distribution maps to illustrate the outcomes.

The main objective of this study is to investigate the impact of variations in road traffic conditions on outdoor air pollution and noise levels in a sousse city center. Firstly, the methodology section will outline the specific urban site chosen for the study and describe in detail the collection of traffic data. It will also explain the use of the French NMPB-2008 model to predict noise levels and the GRAMM/GRAL model to estimate outdoor air pollution levels at the designated site. Secondly, in the results and discussion section, the authors will present and analyse the main findings, including the distribution of road traffic noise and outdoor air pollution levels. Finally, the conclusion summarises the main findings.

II. METHODOLOGY

A. Site description

The research area is located within the governorate of Sousse, positioned along the eastern coastline of the country, approximately 150 kilometers north of the Tunis-Carthage International Airport. It is characterized by high levels of urban traffic and features a diverse mix of residential neighborhoods, educational institutions, cultural hubs, banking facilities, and commercial establishments. Figure 1 provides an overview of the area's layout, highlighting three primary thoroughfares: Mohamed Ali Street (M.A), which facilitates travel from the center of Sousse to neighboring cities such as Monastir, Mahdia, and Sfax; Mohamed V Street, serving as an entry point to the central area of Sousse (M.V); and Habib Thamer Street, which links the urban harbor district to the city center (H.T). Table I illustrates the essential attributes of the study area. These parameters consist of geographical coordinates (latitude: 35°49'31"N, longitude: 10°38'27"E), elevation above sea level (3.51 meters), domain dimensions (376 meters x 626 meters), building heights (ranging from 3 to 12 meters), and road widths (ranging from 3.5 to 7 meters).

TABLE I

SOME PARAMETERS OF THE STUDIED AREA.

Parameter	**Value**
Latitude	35°49'31"N
Longitude	10°38'27"E
Elevation **(**above sea level**)**	3.51 m
Domain dimensions	376 x 626 m²
Building heights	3-12 m
Road widths	3.5-7 m

After obtaining traffic congestion data from Google Maps, map images were processed to create a database of traffic congestion around the harbor area. This database facilitated the analysis of traffic flow intensity along specific routes, with particular attention to the busiest routes and peak hours. Figure 2 illustrates the traffic intensity in the study area during both rush (a) and non-rush (b) hours. By utilizing this data, predictions regarding traffic congestion can be generated, providing valuable insights for individuals making travel decisions and aiding city planners in devising more effective infrastructure strategies.

ISSN: 2356-5608

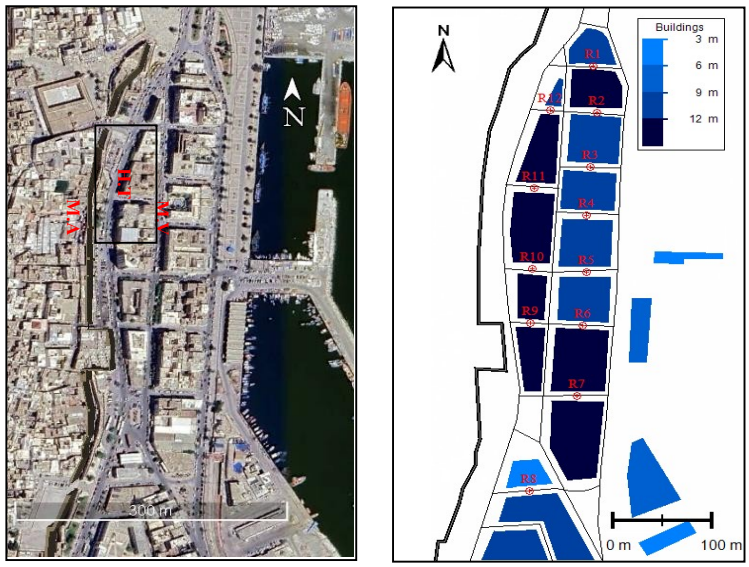

(a) (b)

Fig.1 (a) A top view of the study area from Google Earth and (b) a schematic representation depicting the same study area along with the positions of receptors.

It is important to highlight that the highest levels of particulate matter (PM) were consistently observed along the three busiest streets in the city: Mohamed Ali (M.A), Mohamed V (M.V), and Habib Thamer (H.T) streets.

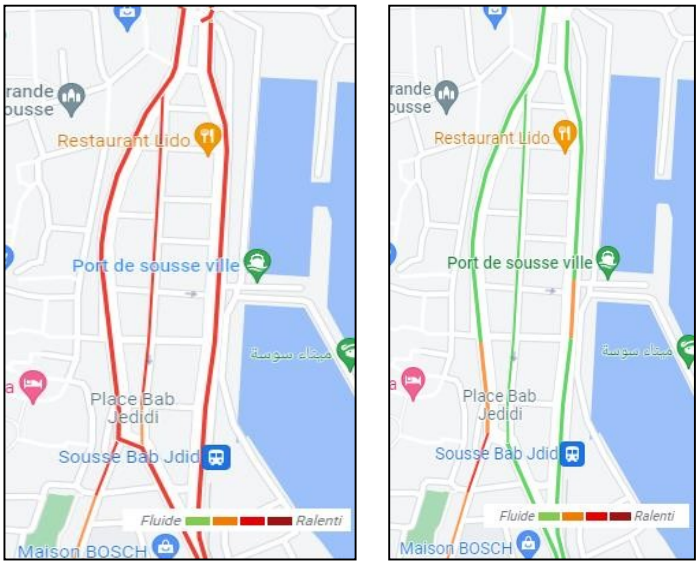

(a) (b)

Fig.2 The traffic volume on the primary roads in the study area depicted during (a) peak hours and (b) off-peak hours.

B. Study flowchart

Our modeling approach follows a three-step procedure using GRAMM/GRAL V22.03 [26], [27]. First, the mesoscale airflow, which takes into account topography and land use effects, is computed by GRAMM for a larger geographical area centered on the city. Secondly, the micro-scale airflow within the city, taking into account the influence of buildings on flow and turbulence patterns, is determined using the GRAL model, driven by the output of GRAMM. Finally, Lagrangian dispersion calculations are performed by the dispersion module of GRAL, guided by

ISSN: 2356-5608

the micro-scale wind fields generated by GRAL. Figure 3 outlines the essential steps required to simulate the dispersion of outdoor road traffic pollution within the GRAMM/GRAL V22.03 environments.

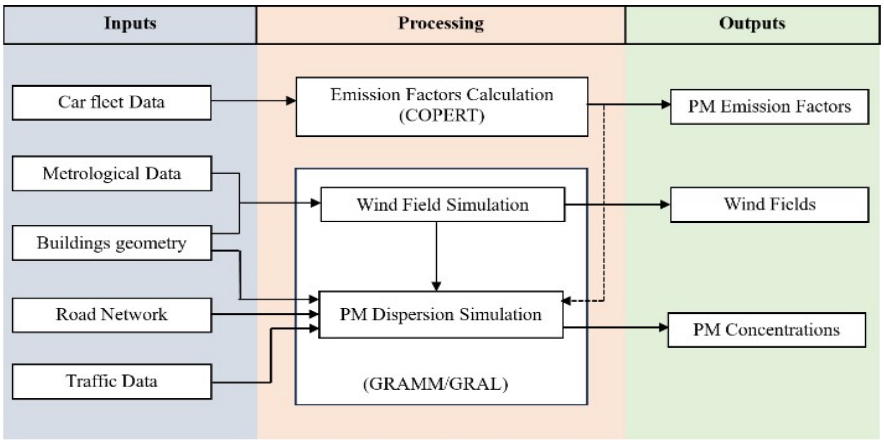

Fig.3 Study flowchart for outdoor air pollution.

Road noise mapping was conducted using cross-platform desktop GIS software, specifically QGIS 3.28.1-Firenze, with the aid of the QGIS plugin OpeNoise 2.0. Developed by the Italian Environmental Protection Agency of Piedmont and released on GitHub in July 2022, this plugin calculates noise levels generated by road sources and generates noise maps employing an interpolation method based on the inverse distance weighting technique. The OpeNoise plugin incorporates the NMPB-2008 model for traffic flow. Essential input data for each road direction includes traffic data, road characteristics like surface type and slope, and building details such as geometry, height, and resident count. The mapping process involves two key layers: one defining buildings and the other defining roads, which serve as the emission sources of noise.

To visualize the road noise simulation using the OpeNoise plugin, we first need to generate a grid to serve as receiver points. Then, we calculate road noise levels for all receivers followed by the creation of contour levels. Finally, we estimate noise exposure using the generated data.

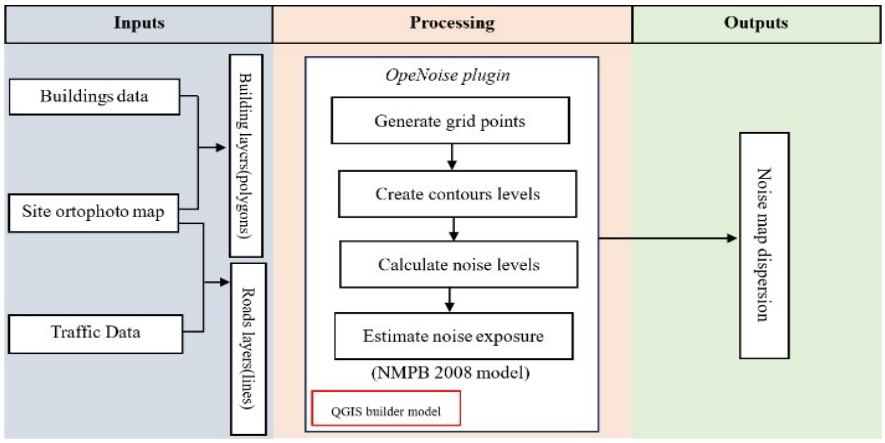

Fig.4 Study flowchart for noise pollution.

C. Modelling Strategy for outdoor air pollution

- *COPERT (Computer Program to calculate Emissions from Road Transport)*

The emission factors for PM2.5 and PM10 particles are computed using the Computer Program to Calculate Emissions from Road Transport (COPERT 5.6.1) [48] package, as described by the following equation:

$$EF_{i,j,k,l} = EF_{H,i,j,k,l} + EF_{T,i} + EF_{B,i} + EF_{R,i}$$

$EF_{i,j,k,l}$ PM total emission factor (g/km.veh),

ISSN: 2356-5608

$EF_{H,i,j,k,l}$ PM hot emission factor (g/km.veh),
$EF_{T,i}$ PM emission factors of tire (g/km.veh),
$EF_{B,i}$ PM emission factors of brake (g/km.veh),
$EF_{R,i}$ PM emission factors of road surface wear (g/km.veh).

When dealing with a heterogeneous vehicle fleet, the average PM emission factor (EFm) is expressed as flows in grams per kilometer per vehicle.

$$EF_m = \sum_{i,j,k,l}(p_{i,j,k,l}. EF_{i,j,k,l})$$

pi,j,k,l represents the proportion of vehicles falling into category i, adhering to emission standard j, utilizing fuel type k, and possessing either an engine cylinder or maximum permissible laden weight l. The emission rate for each road $mi_r(kg/h/km)$, treated as a linear emission source, is then calculated as follows:

$$m_r = \frac{EF_m Q_r}{1000}$$

- *GRAMM/GRAL (Graz* Lagrangian Model)

The GRAL system simulates microscale flows around obstacles, such as buildings, through the resolution of the Reynolds-Averaged Navier-Stokes equations (RANS).

$$\begin{cases} \frac{\partial \bar{u}_i}{\partial x_i} = 0 \\ \frac{\partial \bar{u}_i}{\partial t} + \bar{u}_j \frac{\partial \bar{u}_i}{\partial x_j} = -\frac{1}{\rho}\frac{\partial p}{\partial x_i} + \frac{\partial}{\partial x_j}[\mu_t (\frac{\partial \bar{u}_i}{\partial x_j} + \frac{\partial \bar{u}_j}{\partial x_i}) - \frac{2}{3}\delta_{ij}k] \end{cases}$$

$\bar{u}_i(i = 1, 2, 3)$ represents the mean wind speed components, ρ denotes air density, $\bar{p}$ signifies mean pressure, μt stands for turbulent viscosity and k represents turbulent kinetic energy. The associated turbulence model is (k-ε) :

$$\begin{cases} \frac{\partial k}{\partial t} + \frac{\partial(\bar{u}_j k)}{\partial x_j} = \frac{\partial}{\partial x_j}(\mu_t \frac{\partial k}{\partial x_j}) + P_m + P_b - \varepsilon \\ \frac{\partial \varepsilon}{\partial t} + \frac{\partial(\bar{u}_j \varepsilon)}{\partial x_j} = \frac{\partial}{\partial x_j}(\mu_t \frac{\partial \varepsilon}{\partial x_j}) + \frac{\varepsilon}{k}(1.44(P_m + P_b) - 1.92\varepsilon) \end{cases}$$

Pm and Pb denote the production terms for turbulent kinetic energy attributed to shear stresses and buoyancy respectively, while ε represents the dissipation rate of turbulent kinetic energy.

Lagrangian models are founded on the principle of tracking or tracing particle trajectories within a 3D flow field. According to this principle, the concentration of particles within a volume $dV=d_{x1}.d_{x2}.d_{x3}$ is expressed as:

$$C = \sum_{i=1}^{R} \frac{m_{p,i}}{dV\, t_a} dt$$

where $m_{p,i}$ represents the mass of a single particle, R denotes the total number of integration steps, and ta signifies the averaging time for concentration computation.

- *Road traffic noise model(NMPB-2008)*

The sound levels under favorable conditions ($L_{i,F}$) and homogeneous conditions ($L_{i,H}$) for a given propagation path and octave band are expressed as follows:

$$L_{i,F}(t, i, j, k) = L_{A,w}(t, i, k) - (A_{div}(i, j) + A_{atm}(i, j, k) + A_{sol,F}(i, j, k))$$

$$L_{i,H}(t, i, j, k) = L_{A,w}(t, i, k) - (A_{div}(i, j) + A_{atm}(i, j, k) + A_{sol,H}(i, j, k))$$

Where $L_{A,w}$[dB(A)] represents the sound power level of point source i.

ISSN: 2356-5608

A_{div} The attenuation due to geometric spreading,
A_{atm} The attenuation due to atmospheric absorption
$A_{sol,H}$ The attenuation due to ground effect under homogeneous propagation conditions and for a given octave band.

III. RESULTS AND DISCUSSION

A. Estimation of PM traffic emissions

Traffic emissions were computed utilizing COPERT 5.6.1, which determines road traffic emissions of air pollutants such as PM10 and PM2.5 for each road segment

TABLE II

METEOROLOGICAL CONDITIONS DURING THE TWO OBSERVATION PERIODS. (APRIL 10, 2023).

Parameter	**Rush hour (10^h00-11^h00)**	**Non-rush hour (14^h00-15^h00)**
Wind velocity (at 10 m)	4 km/h	20 km/h
Wind direction	338°	100°
Temperature	19,6 °C	21 °C
Atmospheric pressure	1021,7 hPa	1019 hPa
Relative humidity	33 %	21 %
Cloud cover	0/8 oktas	0/8 oktas
Precipitation	0 mm	0 mm

The necessary input data both during peak and off-peak hours, mainly consist of the percentage distribution of vehicle types (trucks, buses, cars), temporal traffic profiles, meteorological information depicted in Table II [49], road capacity, vehicle fleet characteristics, and the length of each road segment.

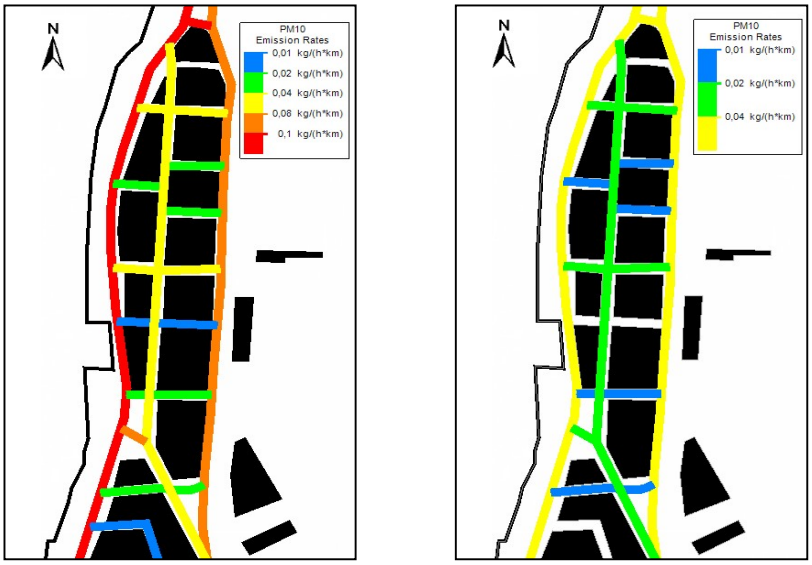

(a) (b)

Fig. 5 PM_{10} emission rates from each road during (a) rush hour and (b) non-rush hour.

Based on the input parameters outlined previously, Figure 5 illustrates the computed traffic emission rates of PM10 and PM2.5 using the Copert 5.6.1 model. It is presumed that, the road's emission rates(kg/h/km) of PM10 during rush hours were ranged from 0.0094 to 0.1467, while during non-rush hours, they ranged from 0.0042 to 0.0660. Similarly, for PM2.5, the emission rates varied from 0.0070 to 0.1092 and 0.0031 to 0.0492 respectively for the rush and the non-rush hours

B. Analysis of Wind Speed

ISSN: 2356-5608

GRAL operates within GRAMM, functioning in diagnostic mode with a 10-meter resolution, contrasting with Berchet et al.'s [26] approach where GRAL operated in prognostic mode at a 5-meter resolution. In diagnostic mode, the flow field around buildings is computed by interpolating GRAMM wind fields on a fine Cartesian grid and assuming a logarithmic wind profile near walls. Mass conservation is maintained by applying a Poisson equation to establish a pressure field for velocity correction. Conversely, in prognostic mode, the flow is explicitly computed through forward integration of prognostic equations. Wind speeds and directions are measured at a height of 2 meters above the ground. Figure 6 (b) illustrates the wind map during non-rush hour. During this period, the highest wind speeds were observed between buildings along Mohamed Ali, Mohamed V, and Habib Thamer streets. However, compared to rush hour, wind speeds were reduced and did not exceed 2 m/s (Figure 6 (a)).

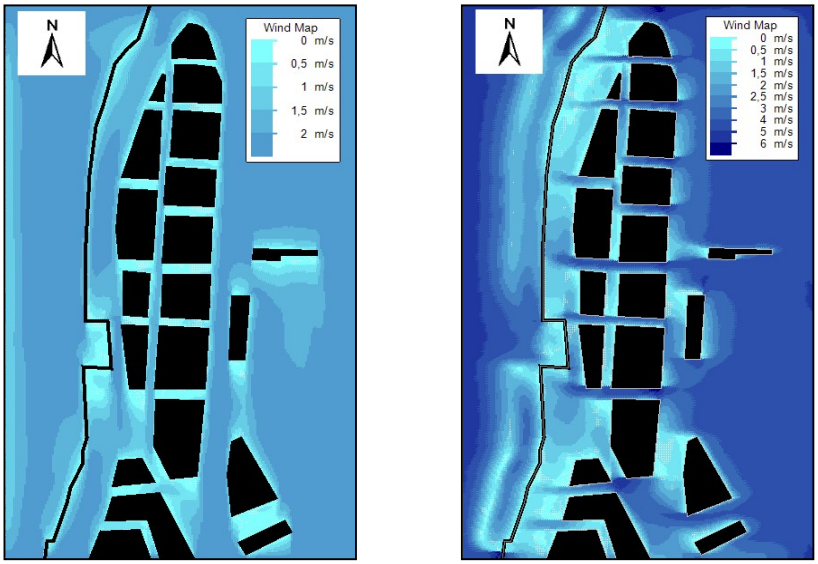

(a) (b)

Fig. 6 PM_{10} emission rates from each road during (a) rush hour and (b) non-rush hour.

C. PM10,PM2.5 modelled dispersion

Mesoscale simulations conducted with GRAMM utilize a horizontal resolution of 2 meters by 2 meters. The vertical concentration grid comprises 9 layers, each with a thickness of 1 meter. Dispersion time is configured at 3600 seconds, with a maximum of 2000 iterations, while the surface roughness remains at 0.8 meters. It's notable that the background concentration of PM10 and PM2.5 is set at 15 and 7.5 micrograms per cubic meter (µg.m-3), respectively. Detailed traffic parameters and road emission rates can be found in Table III.

TABLE III

CONFIGURATION PARAMETERS FOR GRAMM/GRAL SIMULATIONS

Parameter	**Value**	
Horizontal concentration grid	2 m × 2 m	
Vertical concentration grid	9 layers, 1 m per layer	
Dispersion time	3600s	
Maximum iterations	2000 iterations	
Surface roughness	0,8 m	
Background concentrations ($\mu g.m^{-3}$)	$PM_{2.5}$ 7.7	PM_{10} 15
Traffic volumes ranges (veh/h)	Rush hour 155-2410	Non-rush hour 70-1085
Road's emission rates ranges (kg/h/km) $PM_{2.5}$ PM_{10}	Rush hour 0,0070 – 0,1092 0,0094 – 0,1467	Non-rush hour 0,0031 – 0.0492 0,0042 – 0,0660

ISSN: 2356-5608

Figures 7 (a) and (b) reveal notable differences in the spatial distribution of total PM10 concentrations between rush and non-rush hours, with peak levels reaching 30 and 17 (µg.m-3), respectively. Elevated concentrations were predominantly observed in buildings located along the three busiest streets.

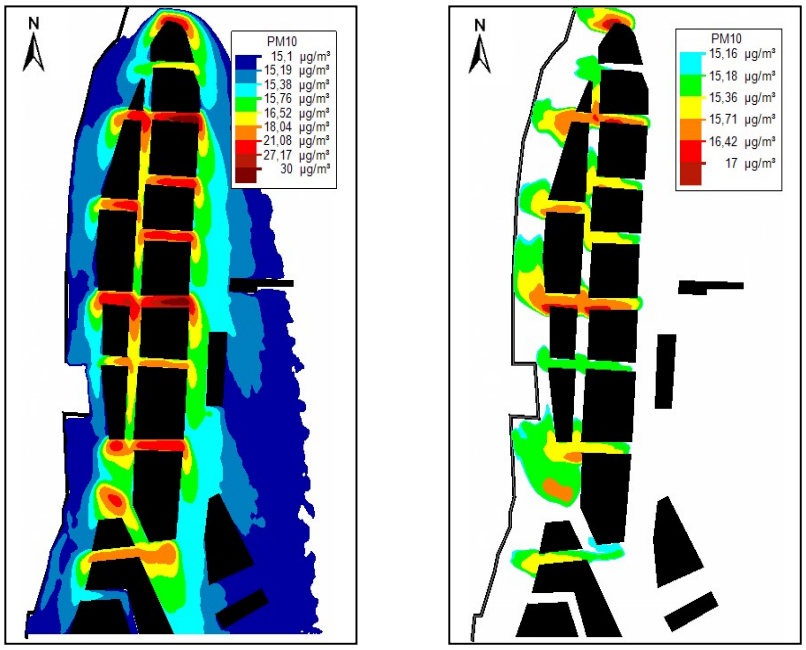

(a) (b)

Fig. 7 PM10 iso-concentration maps at 2m above ground level for (a) rush hour and (b) non-rush hour.

Similarly, in Figures 8 (a) and (b), discrepancies in PM2.5 concentrations between rush and non-rush hours were significant, with maximum values reaching 20 and 10 µg.m-3, respectively. In both scenarios, a substantial proportion of buildings were exposed to outdoor air pollution levels nearing the new EPA standard thresholds of 40 and 25 µg.m-3. It's important to highlight that air pollution from road traffic exceeding these levels is associated with adverse health impacts[50].

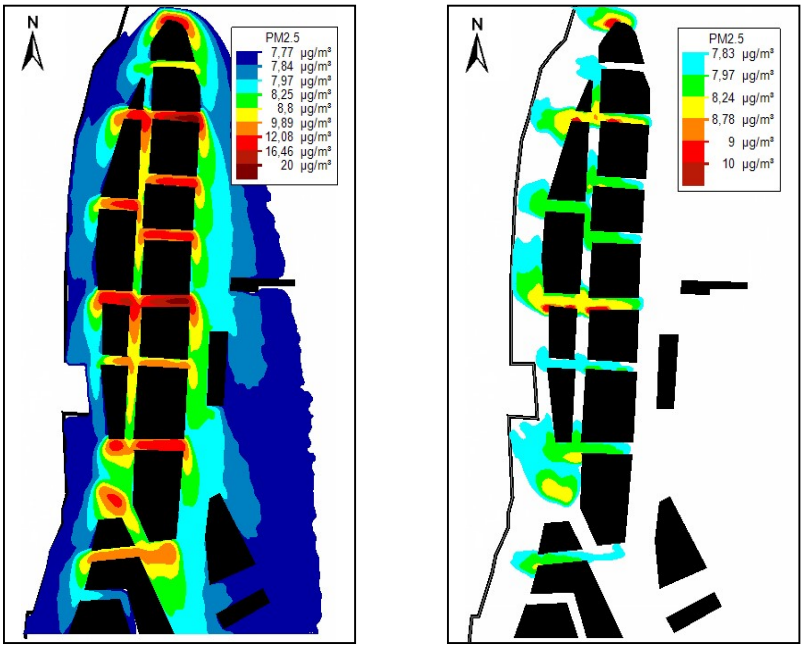

(a) (b)

Fig. 8 PM2.5 iso-concentration maps at 2m above ground level for (a) rush hour and (b) non-rush hour.

ISSN: 2356-5608

In Figures 9 (a) and (b), histograms illustrate the levels of road air pollution exposure during rush and non-rush hours. It's apparent that the most notable disparities in concentration between rush and non-rush hours for both PM10 and PM2.5 were observed at receptor 2, where the maximum levels reached 17 and 13 µg.m-3, respectively. Moreover, individuals residing in close proximity to receptor 2 are subjected to higher levels of road air pollution compared to other residents.

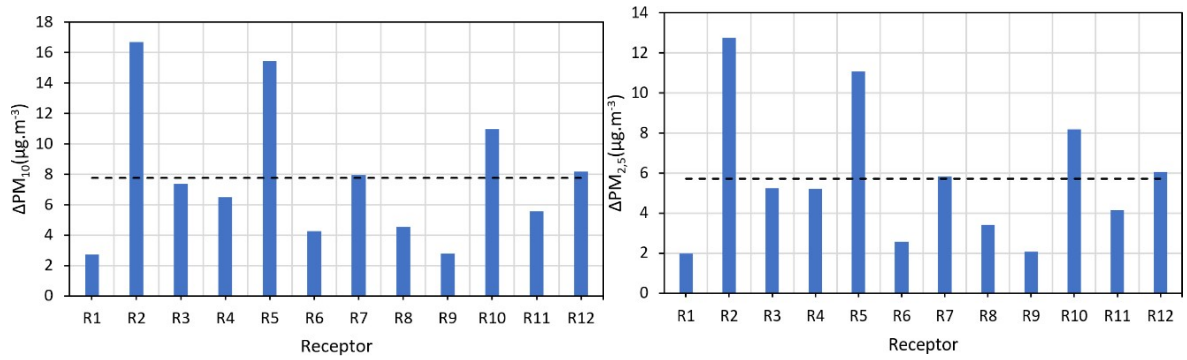

Figure 9 (a) Differences in PM10 concentrations and (b) PM2.5 concentrations between rush and non-rush hours at all receptors.

Figure 10 depicts the PM2.5/PM10 ratios at 2 meters above ground level for each receptor. Elevated PM2.5/PM10 ratio values are typically associated with vehicle-related emission sources, such as exhaust emissions and tire and brake wear, while lower ratios are linked to increased resuspension of road dust due to wearing course abrasion and poor road conditions. Moreover, a high ratio between fine and coarse particulate matter indicates an elevated human health risk level, especially for children, as fine particles (PM2.5) are considered more hazardous and can penetrate deeply into the respiratory system. In this instance, the mean PM2.5/PM10 ratio exceeds 0.5 (0.58), indicating that PM emissions are primarily attributed to exhaust emissions, tire, and brake wear. Additionally, the human health risk level is deemed significant.

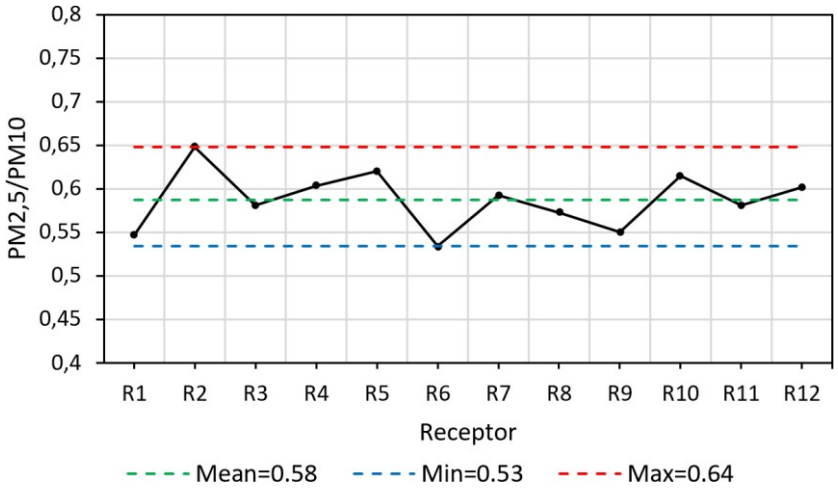

Figure 10 PM2.5/PM10 ratio for all receptors (rush hour).

D. Road traffic noise analysis

Table IV contains the essential parameters for simulating road noise. The simulation utilized a grid size of 57×177=10089 meshes, each with a spatial resolution of 5m×5m. Receptor points were positioned at the center of each mesh, 2 meters above ground level, The road surface is smooth asphalt and flat. Table V also includes traffic for the two hours under study.

ISSN: 2356-5608

TABLE IV

PARAMETERS SET FOR SIMULATING ROAD NOISE.

Parameter	Value
Grid size	57 × 177 = 10089 points
Grid resolution	5 m × 5 m
Receiver height	2 m
Road surface category	Smooth asphalt
Road slope	Flat ≤ 2%

TABLE V

TRAFFIC PARAMETER FOR ROAD NOISE SIMULATION

Traffic parameters	Rush hour	Non-rush hour
Averagespeed ranges (km/h)	20 - 50	50 - 70
Traffic type	Pulsed	Continuous

Figure 11(a) depicts the road noise map during the morning rush hour, highlighting that the most intense road traffic noise was consistently observed along the busiest roads which are Mohamed Ali Street, Mohamed V Street and Habib Thamer Street, streets. Consequently, buildings situated on both sides of these streets are highly exposed to traffic noise levels reaching up to 85 dB(A). Similarly, Figure 11(b) shows the road noise map during non-rush hour periods, In this case, the highest road noise levels were also recorded along TaiebMhiri and Remada streets. However, compared to the rush hour, the noise levels were reduced and did not exceed 78 dB(A). Throughout both hours, the lowest noise levels were observed along the side arteries with the lowest road traffic volumes

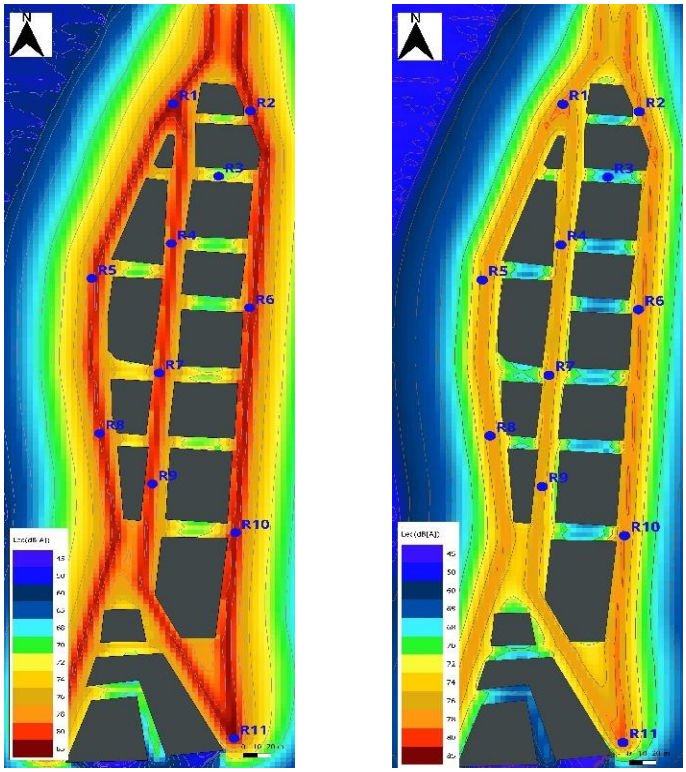

(a) (b)

Figure 11 Noise level contours for (a) rush hour and (b) non-rush hour with receptor's locations

Figure 12 displays the histograms of road noise exposure levels during rush and non-rush hours at 11 receptors, results show that the average road noise level was approximately 3.69 dB(A) when the total traffic volume was reduced by around 45%. This reduction aligns with the findings of the available literature, which stated that road noise levels increase by 3 dB(A) for every doubling of traffic volume [51].

ISSN: 2356-5608

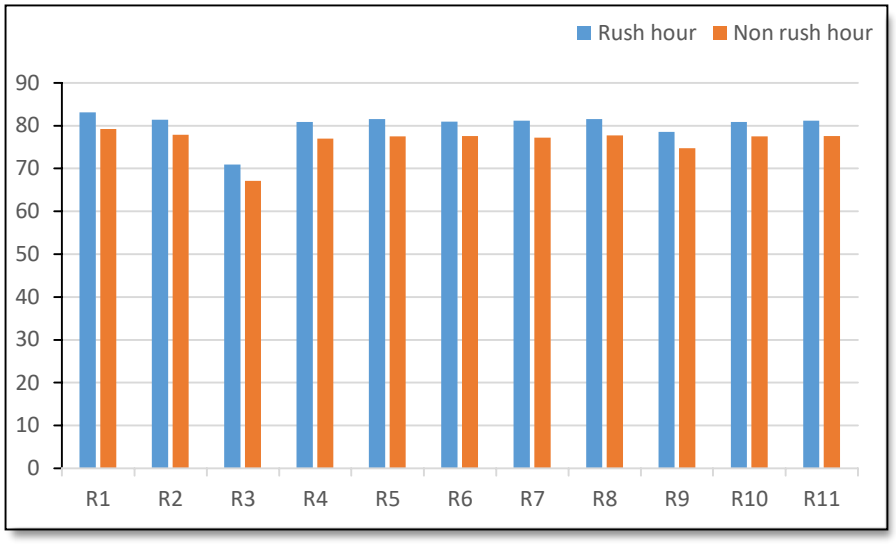

Figure 12 Histograms of road traffic noise exposure levels during rush and non-rush hour

IV. Conclusions

This study explores the relationship between road noise levels, outdoor air pollution, and their combined impact on human exposure at the sousse city center .These environmental factors are known to be associated with various health issues, prompting the investigation undertaken in this paper. Consequently, the following conclusions were drawn from the study:

- PM10 and PM2.5 concentrations exhibit strong correlations with road traffic patterns and atmospheric conditions.
- Pollutants tend to accumulate within street canyons, causing particles to stagnate around buildings.
- Reductions in PM10 and PM2.5 concentrations average at 7.75 µg.m-3 and 5.71 µg.m-3, respectively, with a decrease of 1325 vehicles per hour between rush and non-rush hours.
- Effective traffic management measures show promise in mitigating particle pollution levels, particularly during peak traffic periods.
- Furthermore, road noise simulations conducted using the QGIS environment and OpeNoise 2.0 plugin indicate an average reduction of 3.69 dB(A) in road noise when total traffic volume is decreased by approximately 45% between rush and non-rush hours.

Acknowledgment

The authors express their heartfelt appreciation to all individuals who contributed to the progression of this study, with particular recognition for the committed members of the LESTE laboratory at the National Engineering School of Monastir (ENIM).

References

[1] Web manager center. LE MARCHÉ AUTOMOBILE TUNISIEN, 2021.
[2] KHAN B., JAMIL A., NAWAZ M.S. Effect of Seasonal Variation and Meteorological Parameters on the Environmental Noise Pollution in the Selected Areas of Rawalpindi and Islamabad, Pakistan. Polish Journal of Environmental Studies, 30 (5), 4569, 2021.
[3] FALLAH-SHORSHANI M., YIN X., McCONNEL R., FRUIN S., FRANKLIN M. Estimating traffic noise over a large urban area: An evaluation of methods. Environment International, 170, 107583, 2022.
[4] DJERCAN B., BUBALO-ZIVKOVIC M., LUKIC T., PANTELIC M., MARKOVIC S. Road Traffic Noise Exposure in the City of Novi Sad: Trend Analysis and Possible Solutions. Polish Journal of Environmental Studies, 24 (3), 977, 2015.
[5] YU Y., SU J., JERRETT M., PAUL K.C., LEE E., SHIH I-F., HAAN M., RITZ B. Air pollution and traffic noise interact to affect cognitive health in older Mexican Americans. Environment International, 173, 107810, 2023.
[6] FECHT D., HANSELL A.L., MORLEY D., DAJNAK D., VIENNEAU D., BEEVERS S., TOLEDANO M.B., KELLY F.J., ANDERSON H.R., GULLIVER J. Spatial and temporal associations of road traffic noise and air pollution in London: Implications for epidemiological studies. Environment International, 188, 235, 2016.

ISSN: 2356-5608

[7] Nieuwenhuijsen MJ. Urban and transport planning pathways to carbon neutral, liveable and healthy cities: a review of the current evidence. Environ Int. 2020; 140:105661.
[8] Badland H, Pearce J. Liveable for whom? Prospects of urban liveability to address health inequities. Soc Sci Med. 2019; 232:94–105.
[9] Mueller N, Rojas-Rueda D, Basagaña X, Cirach M, Hunter TC, Dadvand P, et al. Urban and transport planning related exposures and mortality: A health impact assessment for cities. Environ Health Perspect. 2017; 125:89–96. https://doi.org/10.1289/EHP220.M.
[10] EEA. Healthy environment, healthy lives: how the environment influences health and well-being in Europe. 2020.
[11] EEA. Environmental noise in Europe-2020. Eur. Environ. Agency. 2020. https://www.eea.europa.eu/publications/environmental-noise-in europe. Accessed 12 May 2021.
[12] Karner A, Hondula DM, Vanos JK. Heat exposure during non-motorized travel: Implications for transportation policy under climate change. J Transp Health. 2015; 2:451–9.
[13] Md Meftaul I, Venkateswarlu K, Dharmarajan R, Annamalai P, Megharaj M. Pesticides in the urban environment: a potential threat that knocks at the door. Sci Total Environ. 2020;711:134612.
[14] Cao S, Duan X, Zhao X, Chen Y, Wang B, Sun C, et al. Health risks of children's cumulative and aggregative exposure to metals and metalloids in a typical urban environment in China. Chemosphere. 2016; 147:404–11.
[15] WHO. World Health Statistics 2018: Monitoring health for the SDGs. Geneva; 2018. https://apps.who.int/iris/bitstream/handle/10665/ 272596/9789241565585-eng.pdf. Accessed 5 May 2021.
[16] Poom A, Willberg E, Toivonen T. Environmental exposure during travel: a research review and suggestions forward. Health Place. 2021; 70:102584.
[17] Poulsen, Aslak Harbo, et al. « Concomitant Exposure to Air Pollution, Green Space and Noise, and Risk of Myocardial Infarction: A Cohort Study from Denmark ». European Journal of Preventive Cardiology, vol. 31, no 1, janvier 2024, p. 131-41.
[18] Munzel T, Sorensen M, Daiber A. Transportation noise pollution and cardiovascular disease. Nat Rev Cardiol 2021;18:619–636.
[19] Priour.M, Influence des effets couplés de la météorologie et de relief sur la propagation acoustique : utilisation d'une méthode d'éléments finis de frontière et de validation expérimentale, 5 Juillet 2005, 223 pages.
[20] E. Konstantinos Kakosimos, Ole Hertel, Matthias Ketzel, Ruwim Berkowicz, Environ. Chem. 7 (2010) 485– 503. doi:10.1071/EN10070
[21] US EPA "User's guide for the AMS/EPA regulatory model – AERMOD", Office of Air Quality Planning and Standards, Emissions Monitoring and Analysis Division Research Triangle Park, North Carolina, 27711 (2004).
[22] P.E. Benson, CALINE 4: A dispersion model for predicting air pollutant concentrations near roadways. FHWA-CA-TL-84-15, California Department of Transportation, Sacramento, CA (USA) (1984).
[23] CERC, "Atmospheric Dispersion Modelling System (ADMS 4) User Guide version 4.0" (2007).
[24] Lionel Soulhac, Pietro Salizzoni, F.X. Cierco, Richard Perkins, Atmospheric Environment 45 (2011) 7379- 7395.
[25] Almbauer, R. A., Oettl, D., Bacher, M., and Sturm, P. J.: Simulation of the air quality during a field study for the city of Graz, Atmos. Environ., 34, 4581–4594, https://doi.org/10.1016/S1352- 2310(00)00264-8, 2000.
[26] Oettl, D.: Quality assurance of the prognostic, microscale windfield model GRAL 14.8 using wind-tunnel data provided by the German VDI guideline 3783-9, J. Wind Eng. Ind. Aerod., 142, 104–110, https://doi.org/10.1016/j.jweia.2015.03.014, 2015b.
[27] Berchet, Antoine, et al. « Evaluation of High-Resolution GRAMM–GRAL(V15.12/V14.8)NO_{<I>X</I>} Simulations over the City of Zürich, Switzerland ». Geoscientific Model Development, vol. 10, no 9, septembre 2017, p. 3441-59.
[28] K. Yamamoto, "Road traffic noise prediction model ASJRTN-Model 2008: Report of the Research Committee on Road Traffic Noise," Acoustical Science and Technology, vol. 31(1), pp 2-55, 2010.
[29] B. Li, S. Tao, R. W. Dawson, J. Cao, and K. Lam, "A GIS based road traffic noise prediction model," Applied Acoustics, vol. 63(6), pp. 679- 691, 2002.
[30] Sh. Givargis, and M. Mahmoodi, "Converting the UK calculation of road traffic noise (CORTN) to a model capable of calculating LAeq,1h for the Tehran's roads," Applied Acoustics, vol. 69(11), pp. 1108-1113, 2008.
[31] G. B. Canelli, K. Gluck, and S. Santoboni, "A mathematical model for evaluation and prediction of the mean energy level of traffic noise in Italian towns," Acta Acustica united with Acustica, vol. 53(1), pp. 31- 36, 1983.
[32] E. Wetzela, J. Nicolas, Ph. Andre, and J. Boreux, "Modelling the propagation pathway of street-traffic noise: practical comparison of German guidelines and real-world measurements," Applied Acoustics, vol. 57(2), pp. 97-107, 1999.
[33] C. S. Y. Lee, G. G. Fleming, G. S. Anderson, and C. W. Menge, "FHWA Traffic Noise Model, Version 1.0: User's Guide," Federal Highway Administration United States, Tech Rep. FHWA-PD 96-009, 1998.
[34] H. G. Jonasson, and S. Storeheier, "Nord 2000. New Nordic prediction method for road traffic noise," Swedish National Testing and Research Institute, Tech Rep. 2001-10, 2001.

ISSN: 2356-5608

[35] K. Heutschi, “SonRoad: New Swiss Road traffic noise model,” Acta Acustica United with Acustica, vol. 90(3), pp. 548-554, 2004.
[36] T. Suksaard, P. Sukasem, S. M. Tabucanon, I. Aoi, K. Shirai, and H. Tanaka, « Road traffic noise prediction model in Thailand,” Applied Acoustics, vol. 58(2), pp. 123-130, 1999.
[37] Road noise prediction: 2 - Noise propagation computation method including meteorological effects (NMPB 2008), SETRA, Methodologic guide, 2009.
[38] E. Salomons, D. Van Maercke, J. Defrance, and F. de Roo, “The Harmonoise Sound Propagation Model,” Acta Acustica united with Acustica, vol. 97(1), pp. 62-74, 2011.
[39] S. Kephalopoulos, M. Paviotti, F. Anfosso-Lédée, D. Van Maercke, S. Shilton, and N. Jones, “Advances in the development of common noise assessment methods in Europe: The CNOSSOS-EU framework for strategic environmental noise mapping,” Science of The Total Environment, vol. 482–483 (1), pp. 400-410, 2014.
[40] F. Ibili, E. K. Adanu, C. A. Adams, S. A. Andam-Akorful, S. S. Turay, and S. A. Ajayi, “Traffic noise models and noise guidelines: A review,” Noise & Vibration Worldwide, vol. 53(1-2), pp. 65-79, 2021.
[41] H. N. Rajakumara, and R. M. M. Gowda, “Road traffic noise prediction models: A review,” International Journal of Sustainable Development and Planning, vol. 3(3), pp. 257-271, 2008.
[42] N. Garg, and S. Maji, “A critical review of principal traffic noise models: Strategies and implications,” Environmental Impact Assessment Review, vol. 46, pp. 68-81, 2014.
[43] P. R. Nandurkar, M. P. Nawathe, and C. R. Patil, “Study of traffic noise models in the evaluation of traffic noise levels: A review,” International Journal of Engineering Sciences & Research Technology, vol. 4(2), pp. 497-504, 2015.
[44] S. de Lisle, “Comparison of Road Traffic Noise Prediction Models: CoRTN, TNM, NMPB, ASJ RTN,” Acoustics Australia, vol. 44, pp. 409-413, 2016.
[45] J. Khan, M. Ketzel, K. Kakosimos, M. Sørensen, and S. S. Jensen, “Road traffic air and noise pollution exposure assessment - A review of tools and techniques,” Science of the Total Environment, vol. 634(1), pp. 661-676, 2018.
[46] HOU K., LI X., WANG J., ZHANG J. Evaluating Ecological Vulnerability Using the GIS and Analytic Hierarchy Process (AHP) Method in Yan’an, China. Polish Journal of Environmental Studies, 25 (2), 599, 2016.
[47] BORKOWSKI B., CZAJKA I., PLUTA M., SUDERDĘBSKA K. The Conceptual Design of Dynamic Acoustic Maps to Assess Noise Exposure. Polish Journal of Environmental Studies, 25 (4), 1415, 2016.
[48] COPERT 5 Computer programme to calculate emissions from road transport, www.copert 116 versions 5.6.1.org, EMISIA / EEA COPERT 5, (2021).
[49] Infoclimat, http://www.infoclimat.fr/Infoclimat, 2022
[50] Olukanni, D., Enetomhe, D., Bamigboye, G., & Bassey, D. (2021). A time-based assessment of particulate matter (PM2. 5) levels at a highly trafficked intersection: Case study of Sango-Ota, Nigeria. Atmosphere, 12(5), 532.
[51] W. Yang, J. He, C. He, and M. Cai, “Evaluation of urban traffic noise pollution based on noise maps,” Transportation Research Part D: Transport and Environment, vol. 87, pp. 1-14, 2020.

ISSN: 2356-5608